Energy & Environmental Science

www.rsc.org/ees

Volume 5 | Number 12 | December 2012 | Pages 9675–9950

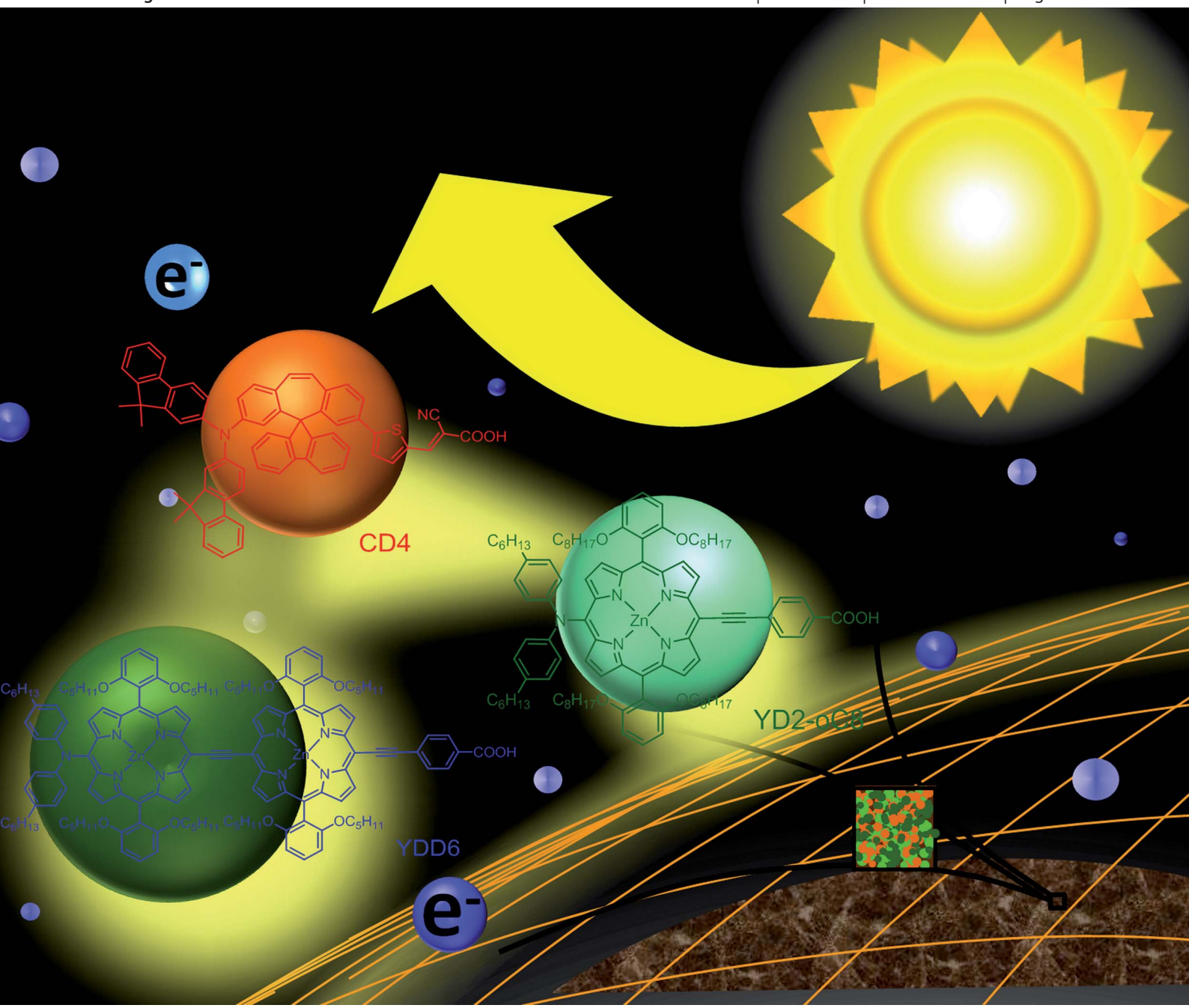

ISSN 1754-5692

RSC Publishing

PAPER

Diau *et al.*

Molecular engineering of cocktail co-sensitization for efficient panchromatic porphyrin-sensitized solar cells

Energy & Environmental Science

Dynamic Article Links

Cite this: *Energy Environ. Sci.*, 2012, **5**, 9843

www.rsc.org/ees

PAPER

Molecular engineering of cocktail co-sensitization for efficient panchromatic porphyrin-sensitized solar cells†

Hui-Ping Wu,[a] Zih-Wei Ou,[b] Tsung-Yu Pan,[a] Chi-Ming Lan,[a] Wei-Kai Huang,[a] Hsuan-Wei Lee,[b] N. Masi Reddy,[b] Chien-Tien Chen,*[c] Wei-Shan Chao,[d] Chen-Yu Yeh*[b] and Eric Wei-Guang Diau*[a]

Received 17th July 2012, Accepted 14th August 2012
DOI: 10.1039/c2ee22870j

Co-sensitization of two or more dyes with complementary absorption spectra on a semiconductor film is an effective approach to enhance the performance of a dye-sensitized solar cell (DSSC). Porphyrin sensitizer YD2-oC8 showed outstanding photovoltaic performance co-sensitized with an organic dye to cover the entire visible spectral region, 400–700 nm. To promote the light-harvesting capability beyond 700 nm, a porphyrin dimer (YDD6) was synthesized for a co-sensitized system. We report a systematic approach for engineering of molecular co-sensitization of TiO_2 films in a cocktail solution containing YD2-oC8, an organic dye (CD4) and YDD6 in a specific molar ratio to optimize the photovoltaic performance of the device. The resulting device showed panchromatic spectral features in the IPCE action spectrum in the region 400–700 nm attaining efficiencies of 75–80%; the spectrum is extended to the near-IR region attaining 40–45% in 700–800 nm region, giving J_{SC}/mA cm^{-2} = 19.28, V_{OC}/mV = 753, FF = 0.719, and η = 10.4% under standard AM 1.5 G one-sun irradiation. This performance is superior to what is obtained from the individual single-dye devices and the two-dye co-sensitized systems. The shifts of TiO_2 potential upon dye uptake and the kinetics of charge recombination were examined through measurements of the charge extraction (CE) and intensity-modulated photovoltage spectroscopy (IMVS), respectively. Five co-sensitized systems were investigated to demonstrate that suppression of dye aggregation of YDD6 in the co-sensitized film is a key factor to further improve the device performance.

[a]*Department of Applied Chemistry and Institute of Molecular Science, National Chiao Tung University, Hsinchu 30010, Taiwan. E-mail: diau@mail.nctu.edu.tw; Fax: +886-3-5723764; Tel: +886-3-5131524*

[b]*Department of Chemistry and Center of Nanoscience & Nanotechnology, National Chung Hsing University, Taichung 402, Taiwan. E-mail: cyyeh@dragon.nchu.edu.tw; Fax: +886-4-22862547; Tel: +886-4-22852264*

[c]*Department of Chemistry, National Tsing Hua University, Hsinchu 30013, Taiwan. E-mail: ctchen@mx.nthu.edu.tw; Fax: +886-3-5711082; Tel: +886-3-5739240*

[d]*Department of Chemistry, National Taiwan Normal University, No. 88, Sec.4, Ding-jou Road, Taipei 11677, Taiwan*

† Electronic supplementary information (ESI) available. See DOI: 10.1039/c2ee22870j

Broader context

Co-sensitization of two or more spectrally complementary dyes on TiO_2 film is an effective approach to enhance the light-harvesting ability for dye-sensitized solar cells (DSSC). Recent report on device performance reaching PCE = 12.3% was based on a co-sensitization system composed of a push–pull porphyrin (YD2-oC8) and an organic dye (Y123) using cobalt-based electrolyte. However, the YD2-oC8/Y123 co-sensitized system harvested solar energy only in the visible spectral region (400–700 nm), leaving rooms for further performance improvement on light harvesting toward the near-IR region. Here, we designed and synthesized a promising near-IR dye, YDD6, a porphyrin dimer that features a broad absorption spectrum extending to 800 nm. However, YDD6 suffers from dye aggregation due to its co-planar structural nature. To solve the aggregation problem for YDD6, we applied a cocktail co-sensitization approach for YDD6 to co-sensitize with YD2-oC8 and an organic dye (CD4). The three-dye co-sensitized device exhibited a remarkable enhancement on overall cell performance, in particular with high J_{SC}, due to a significant improvement of light harvesting in the near-IR region. Five co-sensitized systems according to this promising cocktail approach were investigated and discussed.

Introduction

The increasing demand of sustainable and renewable energy resources has attracted much attention to the development of photovoltaic devices. Whereas silicon-based solar cells require costly production, dye-sensitized solar cells (DSSC) are promising candidates as photovoltaic devices for their advantages of small cost, small mass, coloration and ease of processing.[1,2] Photosensitizers such as ruthenium complexes,[1–5] zinc porphyrins[6–8] and metal-free organic dyes[9–13] serve as efficient light harvesters for DSSC. Advances in co-sensitization of a push–pull zinc porphyrin (YD2-oC8) with an organic dye using a cobalt-based electrolyte boosted the cell performance to $\eta = 12.3\%$,[14] stimulating investigation of the development of new porphyrin sensitizers to improve device performance of DSSCs.

The key structural feature of YD2-oC8 involves long alkoxyl chains in the *ortho*-positions of the *meso*-phenyls so as to envelope effectively the porphyrin ring to decrease the degree of dye aggregation and to block the approach of the electrolyte to the TiO_2 electrode.[14–17] Although the absorption spectrum of YD2-oC8 covers almost the entire visible spectral region, 400–700 nm, the lack of light-harvesting ability beyond 700 nm (near-IR) limits the efficiency of power conversion (PCE) of the device. One strategy to extend the light-harvesting capability of a porphyrin toward the near-IR region is to couple two porphyrin macrocycles through an ethynyl linker, for which the spectra of incident photon-to-current conversion efficiency (IPCE) of the diporphyrin systems were extended to 850 nm.[18,19] The IPCE values of the diporphyrin (YDD0) device were too small, however, to enhance the photocurrent; the performance of this cell was poorer than for its monoporphyrin ref. 18. This poor performance might be due to its nearly coplanar structure that facilitates the formation of dye aggregates that decrease significantly the efficiency of electron injection.

To diminish the extent of dye aggregation from a modification based on the molecular structure of YDD0, in the present work we designed a porphyrin dimer, YDD6 (Fig. 1), for which eight *tert*-butyl side chains in YDD0 are replaced with eight *ortho*-substituted isoamyloxy chains and the *meso*-phenyl opposite to the anchoring group is replaced by a diarylamino group, similar to the molecular design for YD2-oC8 but with the YDD0 diporphyrin core as a light-harvesting center. As such a molecular design failed to solve the aggregation problem for YDD6 (see below), a plausible solution was to resort to co-sensitization.

Co-sensitization of multiple dyes with complementary absorption spectra on a semiconductor film is an effective approach to enhance the light-harvesting property of a DSSC.[20] Many co-sensitization systems are reported to show enhanced photovoltaic performance relative to their individual single-dye systems, which include systems of two or three metal-free organic dyes,[21,22] a black dye co-sensitized with an organic dye,[23,24] phthalocyanine co-sensitized with an organic dye,[25–27] porphyrin co-sensitized with an organic dye,[14,28–30] two mixed porphyrin dyes,[31] and dye co-sensitization in separate layers.[32–34] Robertson stated[20] that the key aspect in molecular co-sensitization is the molar absorption coefficient (ε) of the dye—co-sensitization with strongly absorbing dyes would give sufficient space on the surface of TiO_2 to allow absorption of other dyes with a complementary absorption spectrum; this aspect has been examined in the present work based on co-sensitization of a three-dye system with a TiO_2 electrode fabricated from immersion in a solution containing YDD6, YD2-oC8 and an organic dye (CD4).[35]

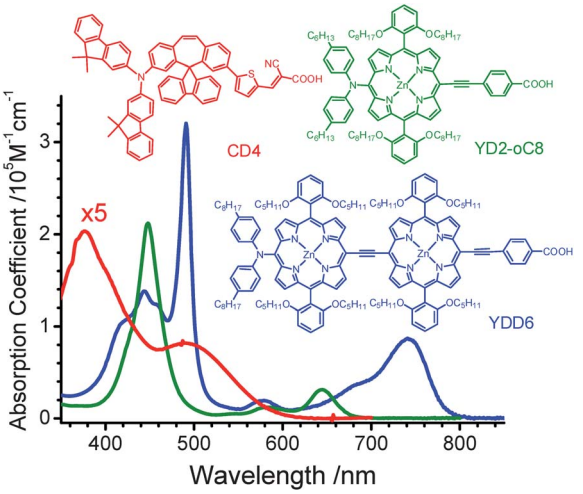

Fig. 1 Absorption spectra of CD4 (red), YD2-oC8 (olive) and YDD6 (blue) in tetrahydrofuran (THF) solution. The corresponding molecular structures are indicated.

Results and discussion

Fig. 1 shows the molecular structures of the three dyes and the corresponding absorption spectra in THF; details of the syntheses of YD2-oC8 and CD4 are published elsewhere[14,35] whereas the synthesis, characterization and electrochemical properties (Fig. S1) of YDD6 are given in the ESI.† Because of the strong coupling between the two porphyrin moieties, the absorption spectrum of YDD6 exhibits a broad split feature for the Soret band (380–550 nm) with a sharp and intense maximum at 491 nm (log ε/M^{-1} cm^{-1} = 5.51); the Q-band absorption comprises a broad feature covering the range 550–800 nm with a maximum at 741 nm (log ε/M^{-1} cm^{-1} = 4.94). The Q band of YDD6 features an intensity of absorption comparable to those of zinc phthalocyanine sensitizers reported for many co-sensitization systems[25–27] but with the tail of spectral absorption extending to the near-IR region (~800 nm). Together with YD2-oC8 and CD4, co-sensitization of these three dyes on the surface of TiO_2 exhibits a panchromatic feature to harvest sunlight in the spectral region 350–800 nm.

DSSC devices were separately fabricated with three individual dyes and with their co-sensitized mixtures adsorbed on TiO_2 films (Fig. S2†), repeated three times using identical working electrodes and a conventional iodide/triiodide electrolyte according to the procedures reported elsewhere;[15,30] the raw data for each *J*–*V* measurement are summarized in Table S1, ESI;† the corresponding averaged photovoltaic parameters are summarized in Table 1. Fig. 2a and b show the current–voltage characteristics (working electrode *a* in Table S1, ESI†) and the corresponding IPCE action spectra, respectively, for devices made of YD2-oC8, CD4, YDD6 and their best co-sensitized composition (labeled D, details follow). Integrating the IPCE of device D (working electrode *a*) over the AM 1.5G solar spectrum

Table 1 Duration of electrode immersion for dye uptake (t), amount of dye loading (DL), and optimized photovoltaic parameters of DSSC fabricated with YDD6, CD4, YD2-oC8 and their co-sensitized mixtures labeled A–E on TiO_2 films of thickness (12 + 9) μm under simulated AM 1.5G illumination (power 100 mW cm^{-2}) and active area 0.16 cm^2[a]

Device composition[b]	t/min	DL[c]/nmol cm^{-2}	J_{SC}/mA cm^{-2}	V_{OC}/mV	FF	η (%)
YD2-oC8	80	143	16.60 ± 0.29	758 ± 3	0.710 ± 0.016	8.8 ± 0.1
CD4	120	238	16.52 ± 0.211	734 ± 7	0.735 ± 0.030	5.8 ± 0.2
YDD6	180	76	9.66 ± 0.84	671 ± 2	0.724 ± 0.602	4.7 ± 0.2
A: 0/5/1	120	0/220/15	15.81 ± 0.36	708 ± 3	0.729 ± 0.022	8.2 ± 0.1
B: 20/0/1	80	118/0/9	18.38 ± 0.26	743 ± 4	0.701 ± 0.008	9.6 ± 0.0
C: 20/5/0	80	123/45/0	16.91 ± 0.25	760 ± 7	0.717 ± 0.020	9.2 ± 0.1
D: 20/5/1	80	115/42/5	19.28 ± 1.21	753 ± 4	0.719 ± 0.020	10.4 ± 0.6
E: 20/5/2	80	103/35/10	18.04 ± 0.47	744 ± 9	0.720 ± 0.020	9.6 ± 0.2

[a] The photovoltaic parameters are averaged values obtained from analysis of the J–V curves of three identical working electrodes for each device fabricated and characterized under the same experimental conditions; the raw data of each J–V measurement are summarized in Table S1, ESI;† the uncertainties represent two standard deviations of the measurements. [b] The molar ratios indicated as YD2-oC8/CD4/YDD6 are mixtures of initial dye solutions before co-sensitization; for systems containing YD2-oC8, the initial solutions comprise [CDCA] = 0.5 mM, [YD2-oC8] = 0.1 mM and other species according to the ratios with respect to [YD2-oC8] for mixtures B–E; for CD4, [CDCA] = 0.3 mM and [CD4] = 0.1 mM; for YDD6, [CDCA] = 0.15 mM and [YDD6] = 0.03 mM; for mixture A, [CDCA] = [CD4] = 0.15 mM and [YDD6] = 0.03 mM. [c] The amounts of dye-loading, indicated as YD2-oC8/CD4/YDD6 for devices A–E, were determined from the desorption of dye molecules on immersion of sensitized TiO_2 electrodes in a basic solution (0.1 M tetrabutylammonium hydroxide in methanol) and the calibrated absorption spectra of each dye.

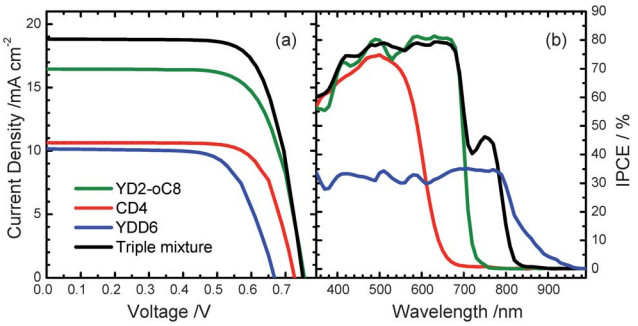

Fig. 2 Optimized photovoltaic properties: (a) current–voltage characteristics and (b) corresponding IPCE action spectra of devices made of YD2-oC8, CD4, YDD6, and the triple mixture (device D) in an optimized ratio with the same fabricated TiO_2 films (12 + 9 μm) under one-sun AM 1.5G irradiation. The device performances of each dye composition were measured based on three identical working electrodes (labeled a–c, Table S1†), but only the results of device a are displayed in the plots.

yields a calculated short-circuit photocurrent density (J_{SC}/mA cm^{-2} = 18.14) slightly less than, but within experimental uncertainties of, that obtained from a J–V measurement (J_{SC}/mA cm^{-2} = 18.81) using a calibrated solar simulator (standard solar spectrum and the integrated values for other devices are given in Fig. S3, ESI†).

The photovoltaic results display a clear trend with the PCE showing the order YD2-oC8 (η = 8.8%) > CD4 (η = 5.8%) > YDD6 (η = 4.7%) for the individual single-dye sensitized devices. The tail of the IPCE spectrum of YDD6 extends much beyond 950 nm, but the overall efficiencies in the region 400–800 nm were too small to provide an advance on photocurrents. When, however, YDD6 was co-sensitized with CD4 and YD2-oC8 on a TiO_2 film with a dye-loading molar ratio YD2-oC8/CD4/YDD6 = 115/42/5 (device D), the overall IPCE values in the 400–700 nm region increased significantly from ~35% to approaching 80%, mimicking the IPCE spectrum of device YD2-oC8 in that spectral region. Furthermore, the IPCE spectrum of the co-sensitized device D includes the near-IR portion, region 700–800 nm, with a maximum at 760 nm attaining ~45%. As a result, device D features J_{SC} (19.28 mA cm^{-2}) superior to that of YD2-oC8 (16.60 mA cm^{-2}), an excellent open-circuit voltage (V_{OC} = 753 mV), similar to that of YD2-oC8 (758 mV), and a satisfactory fill factor (FF = 0.719), increasing the overall PCE to 10.4%, which is 18%, 79% and 121% greater than those of the devices made of individual dyes YD2-oC8, CD4 and YDD6, respectively.

The great performance of device D was an outcome of molecular engineering through systematic co-sensitization of two or three dyes on TiO_2 films in solutions containing each dye at varied molar ratios. To determine the molar ratio of co-sensitization for performance optimization, we investigated five co-sensitized devices, labeled A–E. Device A contained only CD4 and YDD6 in ratio 5/1, device B contained only YD2-oC8 and YDD6 in ratio 20/1, device C contained only YD2-oC8 and CD4 in ratio 20/5, and devices D and E contained all three dyes in ratios 20/5/1 and 20/5/2 of YD2-oC8/CD4/YDD6, respectively. These molar ratios for devices A–E are the recipes for mixtures of the initial dye solutions before co-sensitization. After dye co-sensitization, the amounts of dye-loading (DL) of each dye determined by dye desorption in a basic solution are summarized in the third column of Table 1.

Fig. 3a and b show absorption spectra of the dye-sensitized TiO_2 films in the Soret- and Q-band regions, respectively; these thin-film samples were prepared on immersion of the transparent TiO_2 electrodes (no scattering layers) in dye solutions the same as prepared for the optimized devices. For the absorbance in the 400–500 nm region (Fig. 3a), a systematic trend appears with the order E > D > YD2-oC8 ~B ~C > A > YDD6 ~CD4. The weak absorption of film A (mixture of CD4 and YDD6) in the Soret-band region is due to the small amount of YDD6 adsorbed on TiO_2; the stronger absorptions for film B (mixture of YD2-oC8 and YDD6) and film C (mixture of YD2-oC8 and CD4) are due to the large amounts of YD2-oC8 adsorbed on TiO_2, as both reflected by the data of DL shown in Table 1. For the three-dye systems D and E, the small portions of YDD6 co-sensitized on the TiO_2 films have significantly enhanced the Soret-band

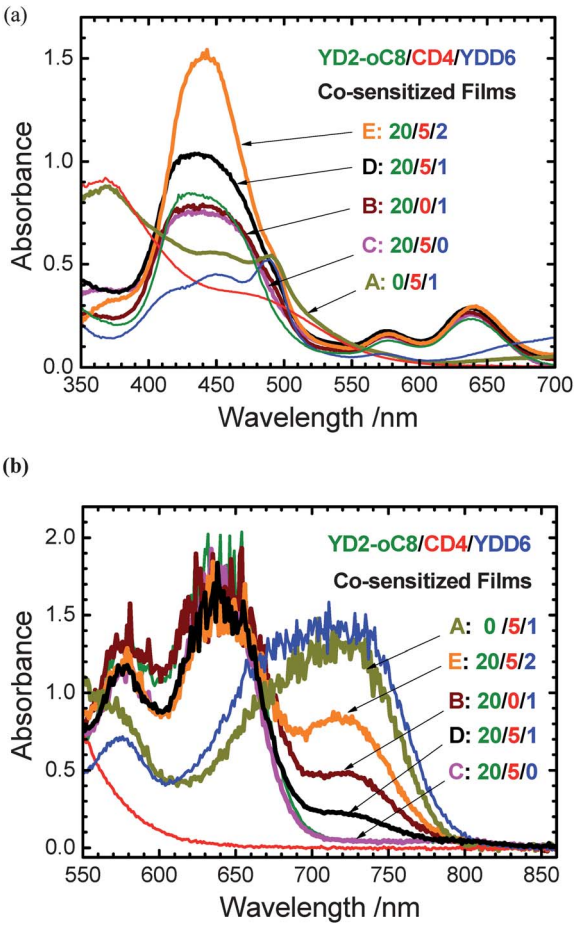

Fig. 3 Absorption spectra of co-sensitized mixtures A–E adsorbed on (a) ~2 μm TiO_2 films (one NP layer with immersion period ~15 min) to show the Soret-band feature and (b) ~12 μm TiO_2 films (two NP and two NR layers with varied immersion periods as shown in Table 1 for optimized devices) to show the Q-band feature. The co-sensitized ratios labeled as YD2-oC8/CD4/YDD6 are the corresponding molar ratios of the three dyes in the solutions for dye uptake on TiO_2 films.

absorption of YD2-oC8 with the absorbance of film E being much greater than the absorbance of film D. The characteristic absorption maxima of YD2-oC8 at 580 nm and 640 nm are almost identical for films B–E (Fig. 3a), manifesting the effect of the strong perturbation to enhance the absorption in the Soret band of YD2-oC8 (400–500 nm) with only a little YDD6 in a three-dye co-sensitization system.

The absorption spectra of the sensitized films in the region 700–800 nm (Fig. 3b) that involve only the Q-band absorptions of YDD6 show a systematic trend of absorbance with order YDD6 > A > E > B > D > C ~ YD2-oC8 ~ CD4 ~ 0, consistent with the corresponding DL that show the same order. The absorption of the YDD6 film decreases greatly from 750 nm to 800 nm with only a tiny absorption tail beyond 800 nm. The IPCE spectrum of the YDD6 device features a long tail from 800 nm broadly extending to ~960 nm (Fig. 2b). The YDD6 aggregates were formed in a single-dye device to produce individuals in the 800–960 nm region, but their absorption features on TiO_2 films were difficult to determine because of the effect of scattered light from the solid films in that spectral region. In the following, we discuss the photovoltaic and kinetic effects of co-sensitization of optimized devices A–E based on results obtained from *JV* characterizations and measurements of IPCE action spectra, charge extraction (CE) and intensity-modulated photovoltage spectra (IMVS). For clarity, the corresponding results are discussed separately: the results of devices A and B are shown in Fig. 4 and results of devices C–E are shown in Fig. 5.

For device A, the photoanode was prepared in a solution containing only CD4 and YDD6 at molar ratio 5/1, which was the best ratio according to the photovoltaic performances of the devices prepared from solutions with varied CD4/YDD6 molar ratios (Fig. S4, ESI†). The performance of device A was optimized to give $\eta = 8.2\%$, which is significantly greater than that of the single-dye device: 5.8% for CD4 or 4.7% for YDD4. The IPCE spectrum of device A exhibits a smooth, YDD6-based spectral feature with the efficiencies smaller than those of device YD2-oC8 in spectral region 400–700 nm. Because the tail of the IPCE spectrum of device A extended to 900 nm, we expect that the aggregation of YDD6 in device A remains a problem that is unresolved. As shown in Fig. 4b, the plots of V_{OC} *vs.* extracted charge densities (N_e) indicate that the TiO_2 potential of device A is located between those of YDD6 and CD4; the plots of electron lifetime (τ_R) *vs.* N_e reveal that device A suffers from serious charge recombination between the conduction-band electrons in TiO_2 and species I_3^- in the electrolyte. V_{OC} and the IPCE values

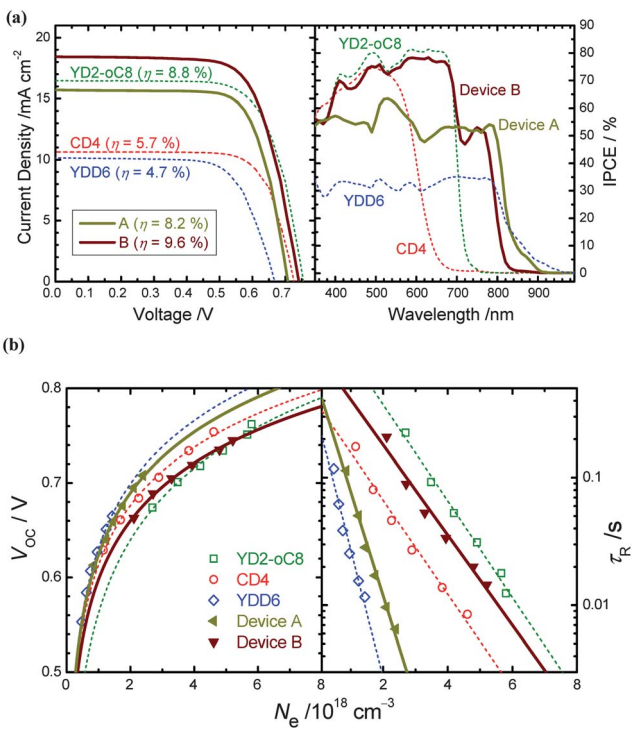

Fig. 4 (a) Current–voltage characteristics (left) and corresponding IPCE action spectra (right) of devices A and B; (b) plots of open-circuit voltage (V_{OC}) *vs.* extracted charge densities (N_e) (left) and of electron lifetimes (τ_R) *vs.* N_e (right) for devices A and B. The corresponding properties of YD2-oC8, CD4 and YDD6 are shown as dashed curves for comparison. The device performances of each dye composition were measured based on three identical working electrodes (labeled *a*–*c*, Table S1†), but only the results of device *a* are displayed in the plots.

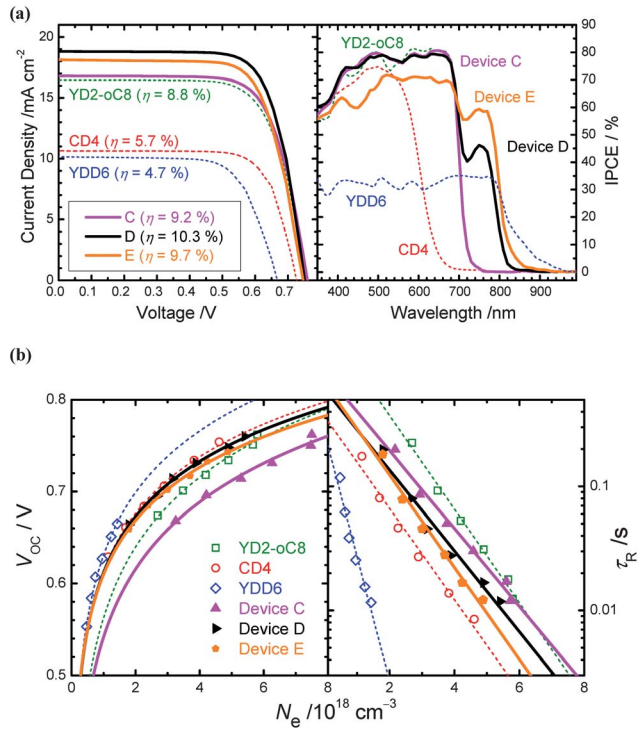

Fig. 5 (a) Current–voltage characteristics (left) and corresponding IPCE action spectra (right) of devices C–E; (b) plots of V_{OC} *vs.* N_e (left) and of τ_R *vs.* N_e (right) for devices C–E. The corresponding properties of YD2-oC8, CD4 and YDD6 are shown as dashed curves for comparison. The device performances of each dye composition were measured based on three identical working electrodes (labeled *a*–*c*, Table S1†), but only the results of device *a* are displayed in the plots.

of device A are consequently between those of their individual single-dye devices. Further promotion of the device performance for the co-sensitization system thus relies on the involvement of YD2-oC8 discussed in the following.

We first consider device B containing only YD2-oC8 and YDD6 prepared in a solution of molar ratio 20/1 (Fig. 4a). The performance of device B was again optimized to give $\eta = 9.6\%$, which is greater than that for device YD2-oC8 ($\eta = 8.8\%$) because J_{SC} is greater for the former than for the latter. The IPCE spectrum of device B displays additional photocurrent responses in region 700–800 nm with maximum efficiency 53% at 750 nm, but the responses in region 400–700 nm are slightly less than those of the YD2-oC8 device. The shoulder of the IPCE spectrum of device B features a blue shift of ~25 nm relative to device A; the edge of the spectral shoulder of B decreases rapidly to zero at 840 nm, which indicates an effective suppression of dye aggregation in device B. V_{OC} of device B is smaller than that of YD2-oC8 (743 *vs.* 758 mV), which is understandable according to the results of plots of V_{OC} *vs.* N_e (similar TiO_2 potentials) and those of τ_R *vs.* N_e (charge recombination more rapid for B than for YD2-oC8) shown in Fig. 4b.

Devices C–E are designed to have the same YD2-oC8/CD4 ratio, 20/5, determined according to the YD2-oC8/Y123 system,[14] but with a varied molar ratio of YDD6 in the dye solutions, designated as 20/5/0 for C, 20/5/1 for D and 20/5/2 for E. After co-sensitization for 80 min, the amounts of dye-loading of both YD2-oC8 and CD4 decreased slightly, but those of YDD6 increased to 5 and 10 nmol cm^{-2} for devices D and E, respectively. Fig. 5a shows the photovoltaic performances of devices C–E, giving the order PCE and J_{SC}/mA cm^{-2} as D (10.4%, 19.28) > E (9.6%, 18.04) > C (9.2%, 16.91) > YD2-oC8 (8.8%, 16.60). The IPCE spectrum of device C shows a flat feature filling the small dip between the Soret- and Q-bands originally existing in the spectrum of device YD2-oC8; such a co-sensitization effect is similar to that reported for the YD2-oC8/Y123 system.[14] For device D, the IPCE spectrum exhibits not only a spectral feature identical to that of device C in region 400–700 nm, but also additional photocurrent response in region 700–800 nm as discussed previously. For device E with double DL of YDD6 relative to device D, the IPCE responses in region 700–800 nm significantly increased to attain a maximum efficiency of ~60% at 750 nm, but the current responses in the 400–700 nm region also decreased by ~10% on average, overall making the J_{SC} of device E smaller than J_{SC} of device D. The IPCE spectral shoulder of device E is red shifted by ~15 nm with respect to that of device D; the spectral edge of device E is extended to ~900 nm, indicative of dye aggregation of YDD6 in device E as discussed above.

V_{OC}/mV also displays a systematic trend for devices in the order: C (760) > YD2-oC8 (758) > D (753) > E (744). The trend of variation of V_{OC} demonstrates the compromises between the shifts of TiO_2 potentials and the retardation of charge recombination shown in Fig. 5b. The upward shifts of potential upon dye uptake show small variations with the order D > E > C > YD2-oC8, but the retardation of charge recombination reflected by τ_R shows an almost opposite trend YD2-oC8 > C > D > E. A greater DL of YDD6 involved in device E hence does not help to up-shift the TiO_2 potential, but it increases the rate of charge recombination to give a smaller V_{OC} than the others.

The long-term stability of the porphyrin-based co-sensitization systems was found to remain stable after 500 h,[30] and performance degradation was only 10–15% in the first 300 h at a low-temperature condition (25–30 °C).[14,30] However, the thermal stability for the devices involving porphyrin sensitizers was always a crucial problem to be resolved. Recent investigation using 8-hydroxylquinoline to replace the conventional benzoic acid as an anchoring group for porphyrin-sensitized solar cells showed excellent stability against solvent desorption.[36] Work is underway to improve the long-term stability for the promising co-sensitization systems reported in the present study.

Conclusions

We have developed a simple co-sensitization approach for molecular engineering of the TiO_2 electrodes in a cocktail solution containing three spectrally complementary dyes, a porphyrin dye (YD2-oC8), an organic dye (CD4) and a porphyrin dimer (YDD6), in an optimized molar ratio to enhance the photovoltaic performance of the device. The objective of such a three-dye co-sensitization is to enhance the light-harvesting power by having YD2-oC8 and CD4 dyes cover the entire visible spectral region (400–700 nm) and by incorporating YDD6 dye to extend the light-harvesting ability toward the near-IR region. With molar ratios controlled for each dye in the solutions, the optimized devices show a panchromatic spectral feature in the IPCE action spectra and attain efficiencies

70–80% and 40–60% in spectral regions 400–700 nm and 700–800 nm, respectively. The optimized device D had amounts of dye-loading/nmol cm^{-2} of 115 for YD2-oC8, 42 for CD4 and 5 for YDD6 in a TiO_2 film of thickness (12 + 9) μm, giving J_{SC}/mA cm^{-2} = 19.28, V_{OC}/mV = 753, FF = 0.719, and PCE = 10.4% under standard AM 1.5 G one-sun irradiation, which is superior to what was obtained from their individual single-dye devices and two-dye co-sensitized systems. The photovoltaic performances of these co-sensitized devices were understood through an analysis of their IPCE action spectra, and by the shifts of TiO_2 potentials upon dye uptake and the kinetics of charge recombination examined through measurements of charge-extraction (CE) and intensity-modulated photovoltage spectra (IMVS), respectively. The best mixture for device D achives ~80% IPCE for the best dye YD2-oC8 absorbing in the 400–700 nm region, but only ~45% IPCE for YDD6 in the 700–800 nm region. The present work indicates that the suppression of dye aggregation for YDD6 in the three-dye co-sensitized system is the key to improve the device performance. With progress using the approach of co-sensitization reported herein, a future challenge is to seek other potential near-IR co-sensitizers with not only a light-harvesting ability extending beyond 800 nm but also less dye aggregation to enhance IPCE above 80%.

Acknowledgements

We thank Professor Chien-Chon Chen for providing the Zahner equipment for CE and IMVS measurements. National Science Council of Taiwan and Ministry of Education of Taiwan, under the ATU program, provided support for this project.

References

1 M. Grätzel, *Acc. Chem. Res.*, 2009, **42**, 1788–1798.
2 A. Hagfeldt, G. Boschloo, L. Sun, L. Kloo and H. Pettersson, *Chem. Rev.*, 2010, **110**, 6595–6663.
3 Md. K. Nazeeruddin, F. De Angelis, S. Fantacci, A. Selloni, G. Viscardi, P. Liska, S. Ito, B. Takeru and M. Grätzel, *J. Am. Chem. Soc.*, 2005, **127**, 16835–16847.
4 C.-Y. Chen, M. Wang, J.-Y. Li, N. Pootrakulchote, L. Alibabaei, C.-h. Ngoc-le, J.-D. Decoppet, J.-H. Tsai, C. Grätzel, C.-G. Wu, S. M. Zakeeruddin and M. Grätzel, *ACS Nano*, 2009, **3**, 3103–3109.
5 Q. Yu, Y. Wang, Z. Yi, N. Zu, J. Zhang, M. Zhang and P. Wang, *ACS Nano*, 2010, **4**, 6032–6038.
6 H. Imahori, T. Umeyama and S. Ito, *Acc. Chem. Res.*, 2009, **42**, 1809–1818.
7 M. V. Martínez-Díaz, G. de la Torre and T. Torres, *Chem. Commun.*, 2010, **46**, 7090–7108.
8 M. G. Walter, A. B. Rudine and C. C. Wamser, *J. Porphyrins Phthalocyanines*, 2010, **14**, 759–792.
9 G. Zhang, H. Bala, Y. Cheng, D. Shi, X. Lv, Q. Yu and P. Wang, *Chem. Commun.*, 2009, 2198–2200.
10 Z. Ning and H. Tian, *Chem. Commun.*, 2009, 5483–5495.
11 Y. Ooyama and Y. Harima, *Eur. J. Org. Chem.*, 2009, **18**, 2903–2934.
12 Z. Ning, Y. Fu and H. Tian, *Energy Environ. Sci.*, 2010, **3**, 1170–1181.
13 Y. Wu, M. Marszalek, S. M. Zakeeruddin, Q. Zhang, H. Tian, M. Grätzel and W. Zhu, *Energy Environ. Sci.*, 2012, **5**, 8261–8272.
14 A. Yella, H.-W. Lee, H. N. Tsao, C. Yi, A. K. Chandiran, M. K. Nazeeruddin, E. W.-G. Diau, C.-Y. Yeh, S. M. Zakeeruddin and M. Grätzel, *Science*, 2011, **334**, 629–634.
15 Y.-C. Chang, C.-L. Wang, T.-Y. Pan, S.-H. Hong, C.-M. Lan, H.-H. Kuo, C.-F. Lo, H.-Y. Hsu, C.-Y. Lin and E. W.-G. Diau, *Chem. Commun.*, 2011, **47**, 8910–8912.
16 C.-L. Wang, C.-M. Lan, S.-H. Hong, Y.-F. Wang, T.-Y. Pan, C.-W. Chang, H.-H. Kuo, M.-Y. Kuo, E. W.-G. Diau and C.-Y. Lin, *Energy Environ. Sci.*, 2012, **5**, 6933–6940.
17 T. Ripolles-Sanchis, B.-C. Guo, H.-P. Wu, T.-Y. Pan, H.-W. Lee, S. R. Raga, F. Fabregat-Santiago, J. Bisquert, C.-Y. Yeh and E. W.-G. Diau, *Chem. Commun.*, 2012, **48**, 4368–4370.
18 C.-L. Mai, W.-K. Huang, H.-P. Lu, C.-W. Lee, C.-L. Chiu, Y.-R. Liang, E. W.-G. Diau and C.-Y. Yeh, *Chem. Commun.*, 2010, **46**, 809–811.
19 Y. Liu, H. Lin, J. T. Dy, K. Tamaki, J. Nakazaki, D. Nakayama, S. Uchida, T. Kubo and H. Segawa, *Chem. Commun.*, 2011, **47**, 4010–4012.
20 N. Robertson, *Angew. Chem., Int. Ed.*, 2008, **47**, 1012–1014.
21 Y. Chen, Z. Zeng, C. Li, W. Wang, X. Wang and B. Zhang, *New J. Chem.*, 2005, **29**, 773–776.
22 D. Kuang, P. Walter, F. Nüesch, S. Kim, J. J. Ko, P. Comte, S. M. Zakeeruddin, M. K. Nazeeruddin and M. Grätzel, *Langmuir*, 2007, **23**, 10906–10909.
23 R. Y. Ogura, S. Nakane, M. Morooka, M. Orihashi, Y. Suzuki and K. Noda, *Appl. Phys. Lett.*, 2009, **94**, 073308.
24 L. Han, A. Islam, H. Chen, C. Malapaka, B. Chiranjeevi, S. Zhang, X. Yang and M. Yanagida, *Energy Environ. Sci.*, 2012, **5**, 6057–6060.
25 J.-J. Cid, J.-H. Yum, S.-R. Jang, M. K. Nazeeruddin, E. Martinez-Ferrero, E. Palomares, J. J. Ko, M. Grätzel and T. Torres, *Angew. Chem., Int. Ed.*, 2007, **46**, 8358–8362.
26 J. N. Clifford, A. Forneli, H. Chen, T. Torres, S. Tan and E. Palomares, *J. Mater. Chem.*, 2011, **21**, 1693–1696.
27 M. Kimura, H. Nomoto, N. Masaki and S. Mori, *Angew. Chem., Int. Ed.*, 2012, **51**, 4371–4374.
28 T. Bessho, S. M. Zakeeruddin, C.-Y. Yeh, E. W.-G. Diau and M. Grätzel, *Angew. Chem., Int. Ed.*, 2010, **49**, 6646–6649.
29 J. Warnan, Y. Pellegrin, E. Blart and F. Odobel, *Chem. Commun.*, 2012, **48**, 675–677.
30 C.-M. Lan, H.-P. Wu, T.-Y. Pan, C.-W. Chang, W.-S. Chao, C.-T. Chen, C.-L. Wang, C.-Y. Lin and E. W.-G. Diau, *Energy Environ. Sci.*, 2012, **5**, 6460–6464.
31 M. J. Griffith, A. J. Mozer, G. Tsekouras, Y. Dong, P. Wagner, K. Wagner, G. G. Wallace, S. Mori and D. L. Officer, *Appl. Phys. Lett.*, 2011, **98**, 163502.
32 H. Choi, S. Kim, S. O. Kang, J. J. Ko, M. S. Kang, J. N. Clifford, A. Forneli, E. Palomares, M. K. Nazeeruddin and M. Grätzel, *Angew. Chem., Int. Ed.*, 2008, **47**, 8259–8263.
33 F. Inakazu, Y. Noma, Y. Ogomi and S. Hayase, *Appl. Phys. Lett.*, 2008, **93**, 093304.
34 K. Lee, S. W. Park, M. J. Ko, K. Kim and N.-G. Park, *Nat. Mater.*, 2009, **8**, 665–671.
35 W.-S. Chao, K.-H. Liao, C.-T. Chen, W.-K. Huang, C.-M. Lan and E. W.-G. Diau, *Chem. Commun.*, 2012, **48**, 4884–4886.
36 H. He, A. Gurung and L. Si, *Chem. Commun.*, 2012, **48**, 5910–5912.

